UKRAINIAN CATHOLIC UNIVERSITY

BACHELOR THESIS

Development of a Small UAV for Bird-Inspired Perching on Large UAVs

Author:
Diana HROMIAK

Supervisor:
Ing. Daniel HEŘT

A thesis submitted in fulfillment of the requirements
for the degree of Bachelor of Science

in the

Department of Computer Sciences and Information Technologies
Faculty of Applied Sciences

УКРАЇНСЬКИЙ КАТОЛИЦЬКИЙ УНІВЕРСИТЕТ

APPLIED
SCIENCES
FACULTY

Lviv 2023

Declaration of Authorship

I, Diana HROMIAK, declare that this thesis titled, "Development of a Small UAV for Bird-Inspired Perching on Large UAVs" and the work presented in it are my own. I confirm that:

- This work was done wholly or mainly while in candidature for a research degree at this University.

- Where any part of this thesis has previously been submitted for a degree or any other qualification at this University or any other institution, this has been clearly stated.

- Where I have consulted the published work of others, this is always clearly attributed.

- Where I have quoted from the work of others, the source is always given. With the exception of such quotations, this thesis is entirely my own work.

- I have acknowledged all main sources of help.

- Where the thesis is based on work done by myself jointly with others, I have made clear exactly what was done by others and what I have contributed myself.

Signed:

_____

Date:

_____

"How about if I sleep a little bit longer and forget all this nonsense."

Franz Kafka

UKRAINIAN CATHOLIC UNIVERSITY

Faculty of Applied Sciences

Bachelor of Science

Development of a Small UAV for Bird-Inspired Perching on Large UAVs

by Diana HROMIAK

Abstract

Unmanned Aerial Vehicles (UAVs) extend their usage to various fields, resulting in increased research in this area. To expand the UAVs' operational working area, different solutions were developed. In this thesis, we designed a passive gripper mechanism inspired by an avian one, which in future will enable UAV transportation by another UAV without the need for energy consumption for transported UAVs. We developed a lightweight UAV with one of the smallest available onboard computers on it. We enabled the UAV to fly autonomously by integrating it into the Multi-Robot Systems (MRS) UAV system and added it to the simulation for further study. We conducted real-world experiments to test the stability of the UAV during autonomous flight and to tune it.

Acknowledgements

I want to express my sincere gratitude to my supervisor Ing. Daniel Heřt, as well as to Ph.D. Tomáš Báča, Ing. Pavel Stoudek, Bc. Murat Ozden and other people from the MRS group for their guidance and support during my thesis. Furthermore, I would like to thank Yuriy Stasinchuk for the opportunity to write a thesis in the MRS group and Denys Datsko for patiently answering all my questions.

Big thanks to my friends, my family, and members of the Ukrainian Catholic University, who helped me to endure this four-year academic journey.

Finally, I would like to thank the Ukrainian army, who courageously defend our country's sovereignty and protect our citizens every day.

Contents

List of Figures

List of Tables

List of Abbreviations

UAV	Unmanned Aerial Vehicle
APM	Automatic Perching Mechanism
ADFM	Automatic Digital Flexor Mechanism
ATLM	Automatic Tendon Locking Mechanism
FPV	First Person View
SLAM	Simultaneous Localization And Mapping
LiDAR	Simultaneous Localization And Mapping
GPS	Global Positioning System
GNSS	Global Navigation Satellite System
IMU	Inertial Measurement Unit
ROS	Robot Operating System
TPU	Thermoplastic PolyUrethane

List of Symbols

ω	angular frequency	rad s^{-1}
a_t, b_t	parameters of a quadratic thrust curve	
T_d	desired thrust on motors $\in [0,1]$	
$\hat{e}_1, \hat{e}_2, \hat{e}_3$	elements of the standard basis	
g	gravitation acceleration	$m\ s^{-2}$
h	UAV heading vector	
η	UAV heading angle	rad

Dedicated to Aida and Milan

Chapter 1

Introduction

1.1   Motivation

The popularity of Unmanned Aerial Vehicles (UAVs) has grown rapidly due to their versatility and flexibility in various applications. They are used for surveying and mapping, aerial photography, environmental monitoring, infrastructure inspection, etc. UAVs are particularly useful in situations where access is difficult or unsafe for humans and where they can perform tasks more efficiently and cost-effectively than ground-based methods or traditional aircraft.

For specific applications, the combination of the UAV's long flight, size and mobility is crucial. While relatively big UAVs can accommodate batteries with more capacity or even additional batteries and large propellers with slower spinning, which is more efficient, small UAVs can carry batteries with limited size and small propellers that have to spin fast, which may require more power, further resulting in a reduction in their endurance and distance of their flight[4]. Therefore, large UAVs can be used for transporting small ones or even be used as a kind of mobile hub, where smaller UAVs can recharge to increase the area of operation and functionality of UAVs.

The ability to land one UAV on another one is a new and unexplored topic that can push the boundaries of what is possible in the field of autonomous systems. By developing a reliable and efficient landing mechanism, it will be possible to expand the capabilities of UAVs and enable them to perform more complex and demanding tasks. This could have significant implications in various fields, such as emergency response, wildlife monitoring, and industrial inspections.

Therefore, developing a novel landing mechanism for small UAVs on larger ones is a critical research topic that can open up new possibilities in the field of autonomous systems.

1.2   Problem statement

A simple approach to UAVs taking off and landing limits the landing surfaces to flat or nearly flat terrain, which can be challenging to apply in areas where such surfaces may not be available, such as sub-UAV landings. In that case, perching can be used as a viable alternative. Perching is a method of landing where the UAV lands on an elevated or vertical surface, such as a tree branch, power line, or wall, and uses its own weight and structure to hold itself in place.

So far, several studies have been conducted on different approaches to perching in dynamic environments, including grasping-based, embedding-based, and attaching-based techniques [13], but none of them was used for on-UAV landing purposes.

This thesis is part of a project which investigates the stability of a bird-like approach to UAV landing on a bigger sub-UAV. Specifically, this work covers the initial stages of designing an attaching mechanism and UAV, testing their reliability, designing a specific UAV with new components, utilizing a new onboard computer, and integrating its model into simulation for further research.

1.3   Thesis structure

Chapter 2 provides a brief overview of the physical characteristics and system specifications of the UAV, including the coordinate system and the pipeline of the used system. In Chapter 3, related works are presented. They are divided into two groups according to their specifics: one on perching studies and the second UAV on UAV landing. Chapter 4 is divided into two parts, describing methods used to design the UAV, and integrating it into the MRS system and simulation. Chapter 5 shows the results of experiments conducted with the developed UAV. Finally, Chapter 6 contains conclusions and a description of future work.

Chapter 2

Background

This chapter describes the technique of UAV perching, the hardware components and the UAV system used in this thesis.

2.1 Birds perching

Birds have an Automatic Perching Mechanism (APM)[3] provided by an Automatic Digital Flexor Mechanism (ADFM) and an Automatic Tendon-Locking Mechanism (ATLM). When a bird bends its legs, the tendons connecting the muscles of its upper leg to its toes extend behind the ankle(2.1), causing the tendons to be pulled and the toes to close due to the action of the ADFM automatically. This enables them to sleep while perching without actively gripping, and when they are ready to take off, they must actively stand up to release their grip.

When transferring this mechanism to the field of robotics, an inelastic string can be used to mimic the mechanism of the bird's tendon, allowing a UAV to hold on to the branch using UAV's mass to create tendon tension for closing gripping claws. For further simplification in the thesis, the string will be referred to as a tendon.
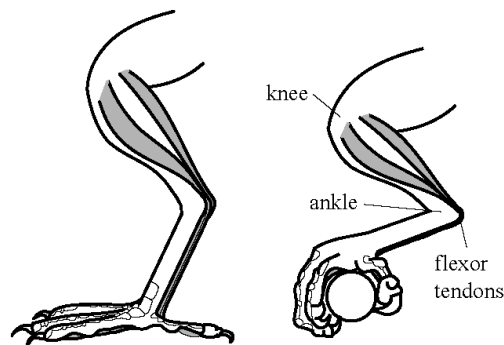
FIGURE 2.1: Illustration of bird's tendon. Taken from [2].

2.2 Classification of UAVs

At the highest level, UAVs can be classified into fixed wings, rotary wings and their hybrids. In this work, the UAVs being mentioned are rotary-winged and use multirotor technology.

Rotary-winged UAVs can be further classified into two types: normal and racing. Normal UAVs are used for general purposes like mapping, transporting, firefighting, etc. They are typically larger and equipped with a variety of sensors, such as cameras, LiDAR, and other specialized equipment, depending on their intended

use. Racing UAVs are light and able to perform aggressive manoeuvres, designed to be fast and agile. They have a smaller frame, powerful motors, and a low centre of gravity, which allows them to accelerate quickly and change direction rapidly. However, they are overpowered and less stable. Because of all these characteristics racing UAVs are mostly used for First Person View (FPV) flights.

2.3 Hardware setup

UAVs are inherently unstable and require active stabilization. In order for a UAV to fly controllably, it requires a flight control unit, also known as the flight controller, which is responsible for stabilizing the UAV and controlling its movements by defining input power on rotors. In this work, the flight controller refers to Pixhawk[1][12], if not stated otherwise.

To enable autonomous flight, a UAV requires an onboard computer in addition to the flight controller. The onboard computer processes data from the flight controller, calculates trajectories, and returns them as an input for the flight controller to follow.

For the computer to calculate trajectory, the 3D position of the UAV is required. To determine the position of the UAV in the real world, a variety of sensors can be used. The Global Positioning System (GPS) is commonly used to determine a UAV's global position. When GPS deny environment, e.g. flying inside buildings or in caves, other systems for determining local position can be used, such as laser Simultaneous Localization and Mapping (SLAMs) or 3D Light Detection and Ranging (LiDARs), which provides 3D position; or cameras, RGB-D cameras, and thermal cameras. For UAV's heading magnetometers are used.

2.4 MRS system

MRS UAV system[1] is an open-source ROS-based platform for autonomous UAV control developed by Multi-Robot Systems (MRS) Group[2] at the Czech Technical University in Prague. Unlike other UAV systems that are mostly limited to simulation, it is designed to be used onboard in real-life scenarios.

2.4.1 Robot Operating System

Robot Operating System[3] (ROS) is an open-source robotics framework for building robotics applications.

At its core, ROS is a middleware layer that provides a messaging system for communication between different software components. This messaging system is based on a publish-subscribe model, where nodes (i.e., packages) publish messages to topics, and other nodes can subscribe to those topics to receive the messages. This allows for a highly decoupled system where different components can be developed independently and communicate with each other through a common messaging system, where each node manages a specific element in a system.

---

[1]https://pixhawk.org/
[2]https://ctu-mrs.github.io/
[3]http://wiki.ros.org/ROS/Introduction

2.4.2 Structure of MRS UAV system
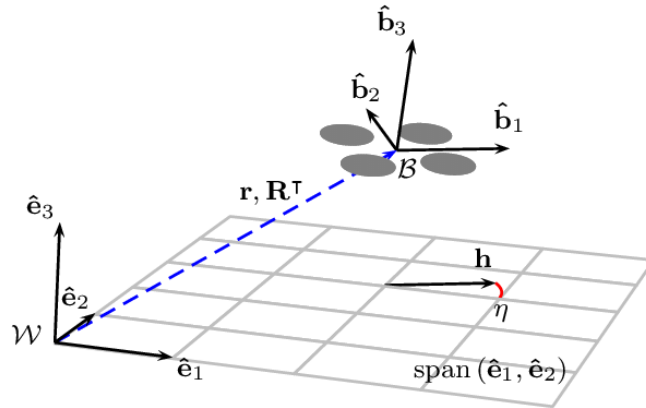
FIGURE 2.2: UAV position in the real-world frame. Taken from [1].

The MRS UAV system has a dynamic model of UAV with a heading-oriented control design.

Figure 2.2 shows a world frame $\mathcal{W}$ with three orthogonal vectors $\hat{e}_1$, $\hat{e}_2$ and $\hat{e}_3$, representing the 3D position and orientation of the UAV body. The body frame $\mathcal{B}$, represented by $\hat{b}_1$, $\hat{b}_2$ and $\hat{b}_3$, is related to the world frame $\mathcal{W}$ through translation ($r = [x, y, z]^T$) and rotation ($R(\phi, \theta, \psi) \in SO(3) \subseteq^{3x3}$, where ϕ, θ, ψ are the Euler angles representing to the yaw, pitch and roll motions of the UAV).

The UAV *heading vector* h is a projection of $\hat{b}_1$ onto the plane spanned by $\hat{e}_1$ and $\hat{e}_2$, forming the heading angle $\eta = atan2(\hat{b}_1^T \hat{e}_2, \hat{b}_1^T \hat{e}_1) = atan2(h_{(2)}, h_{(1)})$ (under the condition of $|\hat{e}_3^T \hat{b}_1| > 0$). Taking that into account, the heading vector and its normalised form, denoted as $\hat{h}$, are defined as:

$$h = [b_1^T \hat{e}_1, b_1^T \hat{e}_2, 0]^T,$$

$$\hat{h} = [cos(\eta), sin(\eta), 0]^T.$$
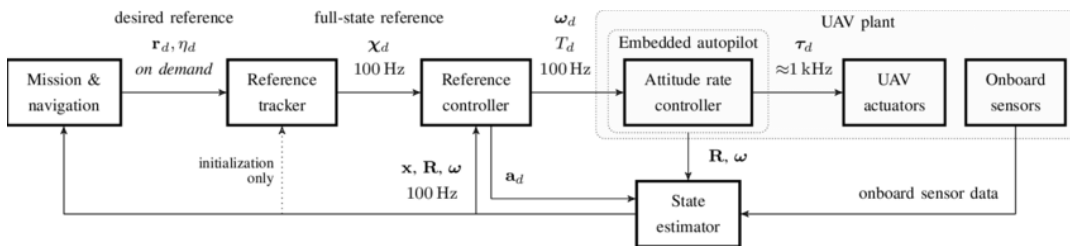
FIGURE 2.3: MRS pipeline. MRS system utilises odometry from all sensors, that is fused on the Pixhawk flight controller by using a Linear Kalman Filter (LKF). Then the mission and navigation software provides the position and heading reference (r_d, η_d) to a reference tracker. The reference tracker then generates a smooth and achievable reference path (χ) for the reference feedback controller. The feedback reference controller uses this path to determine the desired thrust and angular velocities (T_d, ω_d) for the Pixhawk. To estimate the UAV's translation and rotation (x, R), the state estimator combines data from onboard sensors, as well as odometry and localization methods. Taken from [1].

For reference controller, (2.3) MRS system provides two controls for different purposes: SE(3) for manoeuvring flights and Model Predictive Control (MPC) for stable flights(appendix A). Depending on the UAV type, frame, size, motors, and propellers, different controllers with different parameters are used. [21] [5]

For different motors, in order to produce the correct desired thrust and angular velocities, motor parameters should be calculated. Motor speed is controlled by Electronic Speed Controllers (ESCs), they take pulse width modulation(PWM) signal as an input represented in scale [0, 1]. To convert the desired force, calculated by the feedback reference controller, to thrust input on ESCs, we take into account the approximation that desired thrust is directly proportional to squared angular velocity:

$$T_d = a_t \sqrt{f_d} + b_t,$$

a_t and b_t are parameters of a quadratic thrust curve. From there:

$$f_d = mg,$$

where m is the mass of the UAV, and g is the gravity constant. By using those formulas, it becomes possible to calculate the motor parameters during flight tests. This involves obtaining the hover thrust for UAVs with varying additional weights.

2.4.3 Gazebo simulation

For simulation, the MRS system has a simulation environment based on the Gazebo. Gazebo is an open-source, 3D robot simulation software that allows users to create and simulate robotic systems in a virtual environment. Furthermore, it has integration with ROS by using ROS packages with wrappers for Gazebo. Gazebo provides a variety of actuators and sensors, including cameras, GPS, and sonars, which can be attached to the robot models. It simplifies collisions for complex geometries, namely, it does not see the true form of objects but interprets them as basic shapes, such as cylinders or cubes set by user parameters. This approach allows for efficient collision calculations without considering the true form of objects. On the other hand, utilizing visual meshes for collision can significantly complicate Gazebo calculations, resulting in slower than real-time simulations, especially when dealing with complex shapes.

The MRS group has developed simulation models for each of their platforms, thus enabling them to run the simulation alongside the MRS UAV system, effectively creating a Hardware-in-the-loop simulation. Testing UAV trajectories and manoeuvres in a simulation is crucial before attempting them in the real world, although as the simulation is simplified - the results can differ.

Chapter 3

Related work

3.1 Perching approaches

Over the last few years, various approaches to UAV perching on complex surfaces have been developed and experimented with, ranging from simple versions to those more complex, such as inspired by animals like birds[15][18][2] or insects[9][16] or with the use of gripping mechanism inspired by human hand[11]. Given the wide range of surfaces that UAVs may need to land on, this section focuses on works in which UAVs are able to perch on cylindrical objects.

3.1.1 Stereotyped Nature-Inspired Aerial Grasper (SNAG)

W. R. T. Roderick et al. [18] decided to overcome power limitations during environmental monitoring by enabling UAVs to perch on complex surfaces, like brunches. For that purpose, they designed SNAG - a bird-like leg mechanism for UAVs.
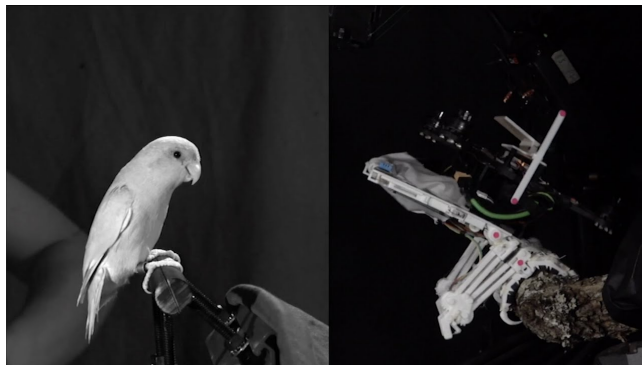
FIGURE 3.1: Similarity between a parrot and SNAG perching. Taken from [18].

In the related to their work research[19], the process of birds perching was divided into a few phases, including aerial, absorption, anchoring, and adjustments, to fixate on branches stably. Unlike this work, the whole process of SNAG landing mimics birds, from its perching trajectory to posture control for balancing itself after perching by moving its centre of mass to the most stable position.

In the aerial phase, birds slow down, prepare their claws, and unfurl their legs. The authors decided to utilize these steps for UAVs to achieve successful perching. They analyzed the speed and angle of birds perching and compared it to UAV parameters. They also focused on expanding and studying the nature of the perching sufficiency region, showing possible angles for stable perching.

The SNAG mechanism implements DFM principles to absorb impact energy through tendon stretching and convert it into squeeze force, resulting in a stronger

grip than actuators alone can provide. Additionally, a quick-release mechanism was added, which resulted in triggering foot close in <17 ms.

The final version of SNAG was inspired by peregrine falcons(anizodactyl), although during its development parrot-like bipedal foot model (zygodactyl) was also studied. The authors decided to stop on falcon's foot, as falcons show impressive grasping performance, can perch on different complex surfaces, and are relatively big, which makes their mass close to UAVs' mass. The claw size and angle between the toes of SNAG were also scaled from birds to make its mass and size as similar as possible to the real one. During their research, they stated that the presence of more toes on the front of the foot would provide more consistent forces to prevent backward slip. This is due to the higher likelihood of engaging with high-quality asperities. However, their experiments show that different finger arrangements (anizodactyl and zygodactyl) show little difference.

As a result of research, they developed bird-like legs, each leg weights 50 g, which has the same percentage with respect to UAV mass as bird legs with respect to bird mass and is capable of wrapping objects in approximately 33-50 ms when landing.

W. R. T. Roderick et al. did an impressive job of studying birds' perching and grasping and trying to apply it to UAVs. Some of their concepts, such as locking mechanisms or making foot fixed, were used in this work, with simplifications for the limitations of this work.

3.1.2 Robot Hand for Ultra-Fast Perching

As mentioned by Andrew McLaren et al. in their research[11], the current methods used for grasping objects with aerial vehicles are slow, inaccurate, and lack adaptability to different objects. As a solution, their paper presents a design for a passive closing, adaptive robot hand that enables ultra-fast grasping of a wide range of everyday objects in aerial environments. The authors state that the developed hand can serve as the end-effector of grasping-capable UAV platforms, offering perching capabilities and facilitating autonomous docking.

The researchers focus on exploring structural compliance in developing simple and adaptive grippers and hands. They propose a quick-release mechanism triggered by a distance sensor, which allows for instantaneous grasping. The hand utilizes only two actuators to control multiple degrees of freedom in three fingers while maintaining superior grasping capabilities even in uncertain object poses or environmental conditions.

The hand achieved a grasping time of 96 ms and a maximum grasping force of 56 N, which allowed them to land the UAV on the pole. Results showed, that a developed hand in one configuration could support up to 3.5 kg, while in the other configuration, it could support up to 5.22 kg. Although this approach has impressive results in perching, it is not used in this work as it is considered overly complex and utilizes active components, which we aim to avoid in this work.

3.2 On-UAV landings

While significant research has been conducted on UAVs landing on complex surfaces, limited literature is available on attempts to transport UAVs by using other UAVs. However, a few studies have explored this concept, with some proposing to use gripping mechanism[14] or landing platform[6] and some using magnets to

create flying modular structures[20]. However, the last one is used for the connected flight of UAVs, and not for transportation.

3.2.1 Flying batteries

Karan P. Jain and Mark W. Mueller[6] introduced a unique approach to a UAV landing in their work, where a smaller UAV equipped with an additional battery was designed to land on a larger UAV for recharging purposes.

The proposed solution uses a mechanical guide structure in the form of a vertical landing platform on the main UAV and landing legs on the flying battery, which allows a fast docking process and simple undocking (regular take-off).

FIGURE 3.2: Top: Main UAV with the docking platform and spring-loaded connectors. Bottom: Flying battery with docking legs and copper plate connectors. Taken from [6].

Similar to this work, the design does not include any active components, reducing power consumption and making it lightweight. Flying batteries use only their own mass to dock and hold on to the main UAV. For that, as mentioned by the authors, zero relative acceleration is required. The requirement for zero relative acceleration between the UAVs was computed using Newton's law, taking into account the mass and acceleration of both the main UAV and the flying battery. The requirement holds as long as the thrust produced by the main UAV is positive and there are no thrust fluctuations. Nevertheless, this docking mechanism allows some lateral play between the vehicles, meaning that the main UAV can perform moderately agile motion while maintaining electrical contact.

The experiment of Karan P. Jain's et al. work results in a 4.7x increase in flight time compared to solo flight and a 2.2x increase over a theoretical limit for the given UAV. However, the experiment did not provide any fixation of smaller UAVs, and the assumption of zero relative acceleration may not hold in all real-life situations, potentially resulting in the fall of the flying battery.

3.2.2   Airborne docking using two multi-rotor aerial robots

Ryo Miyazaki et al.[14] solved the problem of limited flight time in high places or human-restricted areas by developing a system of two multi-rotor UAVs: one transport UAV and another which is transported - called a working UAV. They utilized a bar placed underneath the transport UAV to prevent accidental damage to the working UAV from rotor blades, which can be lowered or raised to mitigate downwash effects. The working UAV is equipped with a dual-gripper robotic hand on its top and has an active vision system that tracks the target, a bar, and autonomously grasps it. The final result of their work can be seen on video[1].

However, a drawback of this system is that the grasping mechanism relies on active components, which may not always be reliable in real-life situations. It could potentially result in the transported UAV being released earlier or later than intended, leading to potential damage to the UAV.

3.3   Gripping mechanisms

Various approaches for making mechanisms for gripping have been made, many of which are inspired by human hands. Some of them utilize a system of rigid-soft parts together with a tendon-driven mechanism[8][10], where soft parts are flexible and allow robotic fingers to bend. Another approach involves the utilization of air pressure to induce finger bending[17]. In this section, we reviewed similar research that adopts a tendon-driven mechanism and incorporates flexible joints to achieve finger bending.

3.3.1   An Adaptive Actuation Mechanism

George P. Kontoudis et al.[8] worked on the design of a finger for anthropomorphic robot hands. Their proposed solution utilizes tendon-driven actuation with two actuators to achieve flexion/extension and adduction/abduction movements at the joint of the fingers.

The paper focuses on modelling and analyzing the actuation mechanism, determining design parameters for desired abduction angles, and establishing a model for spatial motion. Static balance analysis was conducted to compute tendon forces, and a model calculated the stiffness of joints' rotation.

The proposed mechanism uses hybrid deposition techniques. The mechanism was tested by assessing friction, computing the reachable workspace, evaluating force exertion capabilities, demonstrating feasible motions, and evaluating grasping and manipulation abilities.

As a result of their work, the proposed actuation mechanism was fabricated and incorporated with an anthropomorphic robot hand, and its performance was assessed. Their hand resulted in grasping objects with different forms and even performing some manipulations with them.

Similar to their work, our approach also utilizes a tendon-driven mechanism to enable the bending of a soft-rigid finger. While the proposed adaptive actuation mechanism uses actuators to generate forces and allows for both flexion and abduction motions, our focus is on a simplified design using a single tendon for the finger, or "toe" as referred to in this work. The simplified design serves the specific purpose of gripping a pole and thus has a different approach.

---

[1]https://www.youtube.com/watch?v=Gs2YqO1dNSA&ab_channel=ShimonomuraLab

3.4 Conclusions

There are not many works on perching UAVs on another UAV. However, all of them employ active components, which results in power consumption and reliability concerns. In this work, we aim to integrate the findings from previous research on landing UAVs on complex surfaces and focus on designing a solution that addresses power consumption, and fixation aspects to ensure safe and effective perching on another UAV.

Chapter 4

Method

This chapter describes the design of a light-weighted autonomous UAV and a gripper mechanism, which will allow it to perch on another UAV without using any additional power for grasping.

4.1 UAV and gripper design

4.1.1 UAV design

Although the MRS CTU group already has a wide variety of reliable UAV platforms[4], a specific UAV was developed for this work.

Frame

The Carbon Fiber Rotorama Spectre $280x200$ mm frame, which is intended for building a lightweight racing UAV, was used as the base. That makes it a UAV with the smallest frame with the MRS system on it. Non-suitable parts of the default frame were replaced by 3D printed ones, such as holders for the flight controller and onboard computer, to make the UAV as light as possible and utilize all the free space left on the frame.

Flight control

As the MRS system is compatible with Pixhawk, it was used as a flight control unit. Instead of using Pixhawk 4, as on most MRS UAVs, Pixhawk 4 mini was utilized. It differs from Pixhawk 4 in a smaller size resulting in fewer available ports and fewer parameters. It has the same Flight Management Unit (FMU) processor and memory resources as the Pixhawk 4, which allows it to run PX4[1] – the open-source autopilot.

Onboard computer

The onboard computer is used to execute custom localization systems and state estimators while providing low-level control commands to the flight controller.

In the MRS group, most UAV platforms are equipped with Intel Next Unit of Computing (NUC) onboard computers[2]. However, for this work, Khadas VIM4[3] was chosen instead. The Khadas VIM4 is a relatively new mini-computer known for its compact form factor and powerful performance. In comparison, the NUC footprint is typically around 100 x 100 x 30 mm with a weight of approximately 200

---

[1] https://px4.io/
[2] https://www.intel.com/content/www/us/en/products/details/nuc/boards/products.html
[3] https://www.khadas.com/vim4

g (without box assembly)[4], whereas the VIM4 measures 82.0 x 58.0 x 11.5 mm and weighs 67.75 g.

VIM4 is equipped with a 2.2GHz Quad-core ARM Cortex-A73 and a 2.0GHz Quad-core Cortex-A53 CPU, with a 32-bit STM32G031K6 microprocessor and Mali G52MP8(8EE) 800Mhz GPU.

VIM4 also differs from NUC in performance characteristics, while NUC uses x86 Intel Core, Khadas uses an ARM processor, which requires some additional libraries for the functionality of the MRS system. ARM processors are designed for efficient and low-power consumption performance, while Intel Core processors are known for their high-performance capabilities with multiple cores, threads, and advanced features. Both computers support Linux, which is required by the MRS system.

VIM was compared with one of the NUC models used on MRS UAVs, Raspberry Pi 4, which is also considered small-sized.

Characteristic	VIM4	NUC10i7FNK	Raspberry Pi 4
Processor	Amlogic A311D2 (4xCortex-A73, 4xCortex-A53)	Intel Core i7-10710U	Broadcom BCM2711 4x ARM Cortex-A72
RAM	8 GB	max 64 GB	max 8GB
Memory types	LPDDR4X 2016MHz	DDR4-2666 1.2V SO-DIMM	LPDDR4-3200 SDRAM
Storage	32 GB eMMC 5.1, MicroSD card, M.2 NVMe via external breakout board	max 2TB HDD, or 4TB SSD	max 64 GB SD card
Ports	USB2, USB3, HDMI2.1, USB-C, Ethernet	USB-A, USB-C,3xUSB3.1, 2xUSB2.0 HDMI2.0, Ethernet	2xUSB3, 2xUSB2, 2xmicro HDMI, Ethernet, USB-C MIPI DSI, MIPI CSI
Size	82.0 x 58.0 x 11.5 mm	117 x 112 x 38 mm	85.6 x 56.5 x 11 mm

TABLE 4.1: Comparison of Characteristics for VIM4, Raspberry Pi 4, and NUC10i7FNK Computers

The Khadas VIM4, chosen for this work, shows several advantages over other considered computers. VIM4 is more powerful than Raspberry Pi and remains more energy-efficient than the NUC. Although NUC has an advantage in performance, VIM4 has an astonishing form factor, which makes it more suitable for a small UAV, for which NUC will be too large. One notable advantage of the VIM4 is its storage capability. It features 32 GB eMMC 5.1 flash memory, which enables faster read/write operations compared to the Raspberry Pi's MicroSD card. Additionally, the VIM4 supports storage expansion through a MicroSD card and M.2 NVMe via an external breakout board.

Furthermore, the VIM4 is equipped with a fan, ensuring efficient cooling and mitigating the risk of overheating issues commonly experienced with the Raspberry Pi. In addition, Khadas provides comprehensive sources for their products, including code, schematics, 3D models, and more, which makes way for customization and integration.

Measurement sensors

For autonomous perching on bigger UAVs, precise measurements are required. High levels of precision can be achieved using LiDARs or SLAMs, they often provide sub-centimetre precision. However, they are large and cannot be carried by the designed UAV, thus, as an alternative, GNSS and a camera were used. GNSS in good conditions, e.g. good weather conditions, and shielding from the radio-magnet field, etc, can provide accurate positioning information for outdoor environments, while cameras can be used for visual-based localization and mapping. Pixhawk provides a

---

[4]https://www.intel.com/content/www/us/en/support/articles/000005545/intel-nuc.html

GPS module with all the needed configurations. Moreover, some additional sensors are provided with Pixhawk 4, such as a gyroscope, barometer, and accelerometer.

Power supply

LiPo battery with a capacity of 1800mA with four cells was used as a power supply and a Holybro Pixhawk 4 Power Module (PM07) to distribute power on motors and Pixhawk. To accommodate the power requirements of the VIM4, which is 16V, a Buck-Boost was added to step up the voltage, as the maximum output from the distribution board is 5V. The computer is not directly powered from the battery to avoid potential damage caused by unstable voltage.

4.1.2 Gripper design

As one of the aims of this work is to make the endurance of the UAV as long as possible, it was important to make the gripper mechanism light and without any active components, such as motors or actuators.

Removing active components plays an important role not only in power consumption, but also in the reliability of the mechanism. Sensors may fail during the gripping process, which could potentially result in a UAV damage or a crash. Meanwhile, relying solely on physics can provide a secure grip, but it also requires more precise measurements and careful design of the gripper.

Tendon part

To mimic the functionality of a bird's ADFM, a specific joint (analogue of a bird's ankle) was designed. The joint(4.1) contains two gears which enable symmetric bending at the ankle of the lower and upper parts of the leg. The tendon, which is bent around both of them, will shrink approximately one-fourth of the circumference of each of the gear lengths when the leg is bent. As a result, the change in tendon length Δl can be calculated using formulas of arcs length:

$$\Delta l = 2(2\pi r(270/360)) - 2(2\pi r(180/360)),$$

where r is the radius of the gear on which the tendon is bent.

Only gears' radii contribute in Δl, otherwise, the length of the tendon should be proportional to the length of the leg, which can be chosen optionally with respect to the UAV size. However, the length of the leg is important in order to maintain stability during flight, as longer legs may change the moment of inertia of the UAV and make UAV more jittery. At the same time, a longer leg increases torque, which transfers to a stronger grip.

The upper and lower parts of the legs were chosen to have identical lengths in order to keep the centre of mass above them. The maximum angle between the legs was set to 156 degrees. This constraint disables the legs from bending into different sides while perching, ensuring that the legs maintain a specific alignment.
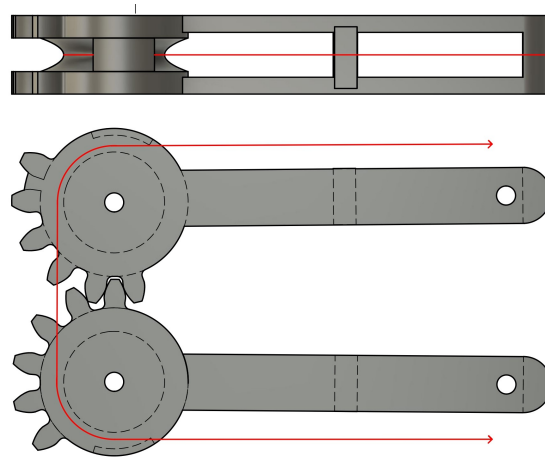
FIGURE 4.1: Design of leg joint. The tendon path is marked in red colour.

Gripper

The gripping mechanism of the system was also inspired by ADFM, with additional simplification due to the limitations of its task. To enable adaptability to grip a pole, it is constructed using small 3D printed pieces (segments) that are connected together using a flexible material made of Thermoplastic Polyurethane (TPU), which is also 3D printed. This design was chosen for its simplicity and availability of 3D printers. Other solutions, such as using fully rubber segments that require cutting of rubber, were also considered. However, the 3D printed design with TPU segments was a more practical and effective solution. A group of three segments and joints forms a soft-rigid toe (4.2).
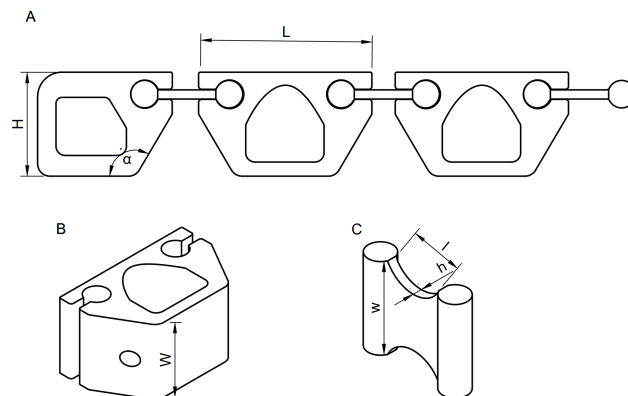

FIGURE 4.2: (A) Toe sketch on the top. (B) 3D sketch of a segment; (C) 3D sketch of a flexible joint.

To properly design flexible joints between segments, their stiffness must be taken into account, as it will determine the force needed to be applied in order to bend a toe. For that correct length, height and width of the joint should be chosen, as the UAV is lightweight and creates small force from its mass ($F_m = mg$, where m is the mass of the UAV and g is the acceleration due to gravity).

The axial stiffness of the joint can be calculated as:

$$k = \frac{EA}{l}.$$

Where E is Young's modulus (or elastic modulus), A is the cross-section area of the joint, which can be simplified to the area of a rectangular prism, and L is the length of the joint. Young's modulus is:

$$E = \frac{\sigma}{\eta} = \frac{F/A}{dl/l}.$$

Where σ is uniaxial stress, η is strain, F is the force exerted on a joint, and dl is the change in the length. According to the formula, stiffness is directly proportional to the cross-section and inversely proportional to the length of a joint. To simplify calculations, Young's modulus of the used TPU material was not determined, and the stiffness of the joints was specified based solely on those proportions.

Making joints with different stiffness can result in bending segments at different angles within a given unit of time. This can be used for gripping complex surfaces. However, in this particular work, the task was to grip a cylindrical pole, and therefore all the joints were designed with the same stiffness.

The absence of additional servo motors or sensors in the gripper results in its reliance on the joint's elastic force to unbend the toe and release the pole when the UAV takes off. This behaviour occurs due to the thrust of the motors causing the legs to unbend, leading to the loosening of tendons connecting each segment and joints made of TPU tend to return to their initial position.
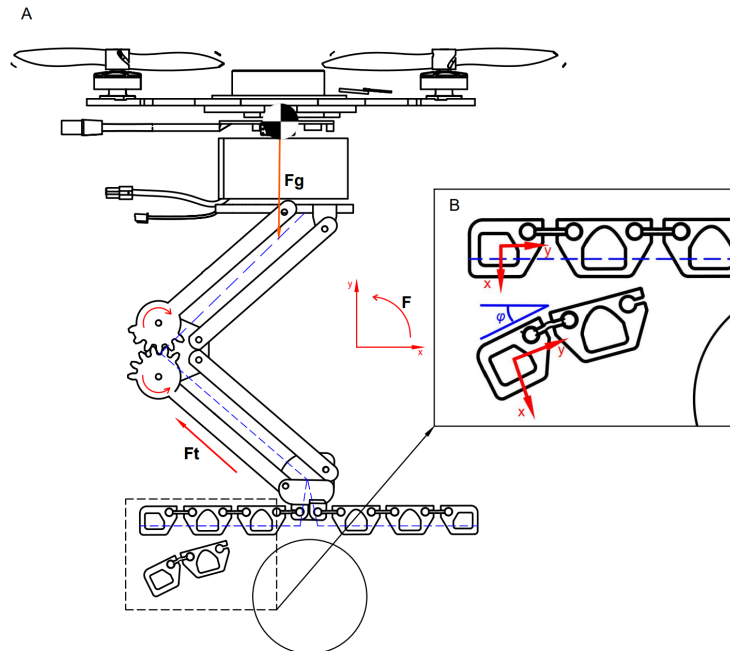

FIGURE 4.3: UAV model. (A) The tendon path is marked in a blue dashed line. F_g gravity force on UAV, F_t tendon tension. (B) Toe bending and deflection of flexible joint: φ angular displacement of the segment, due to tendon pull and flexion of the joint. In addition to the tendon pull, gravity exerts a force on each segment, which also causes fingers to bend.

To simplify the control of the centre of mass without the use of servo motors, both the gripper and UAV were designed to maintain a fixed orientation with respect to the leg by the use of additional supports, which are shown in Figure 4.3.

4.2 Integration of the UAV into the MRS system

In order to make the UAV fly autonomously, the MRS system was installed on the onboard computer. As the UAV utilize a racing platform, a flight controller was set up with specific parameters for racing UAVs. Afterwards, it required creating configurations in the MRS system, which included the MPC controller, MPC tracker and SE(3) controller gains, as well as parameters related to the UAV weight estimation, land and take-off tracking, battery characteristics, etc.

For this particular UAV, the SE(3) controller was selected due to its exceptional manoeuvrability and responsiveness [1](Appendix **??**). That makes its movement look sharper while maintaining enough precision for perching.

Following the initial setup, the UAV should be tuned during flight to optimize its performance. This iterative process involves tracking the UAV's performance and making corrections in gains as needed. Fine-tuning the gains allows to enhance the UAV's stability, compensates for air resistance effects on the long legs, and improves its precision for autonomous perching operations.

4.2.1 Motor parameters estimations

One of the most important parameters to calculate before a flight is motor parameters (a_t, b_t), as they will determine the thrust of the UAV. To calculate motor parameters without conducting real flight testing, it is sufficient to know the maximum thrust per motor (motor constant), which is specified for each motor with certain propellers. The hover thrust, required for determining motor parameters, can be calculated by considering the desired thrust and utilizing known parameters from Pixhawk. These parameters, combined with a selected set of realistic masses, enable the scaling of the desired thrust to a thrust value within the range of [0, 1].

Further, motor parameters have to be calculated during real flight, where real mass and thrust are known.

4.2.2 MRS simulation with Gazebo

In order to incorporate the UAV model into the Gazebo simulation environment, several steps need to be taken.

For its visualisation, the 3D model of each part of the UAV was designed and provided to the simulator as a mesh. Additionally, non-static components, such as motors, or components that do computations, such as Pixhawk, or sensors, should be provided with plugins.

To simulate the physics of motors, the thrust and torque are calculated as follows:

$$T = \omega^2 K_F,$$

$$\tau = T K_T.$$

Where T is thrust, ω is the real angular velocity, τ is torque, K_F is motor constant, and K_T is moment constant. For that, constants for specific motors should be provided. Here again, the motor constant is used.

In the simulation, collisions involving the UAV are simplified by treating it as a basic shape, such as a cylinder. For its area calculation, the arm's length and the height of the UAV should be taken into consideration.

Legs simulation

As Gazebo simplifies physics, the focus is not on replicating the exact mechanics of the legs, as that would require developing an additional plugin and not showing the real result. Thus, they are represented as always unbent and simplify their collision to the cylinder of approximately their size.

Moment of inertia

To create a precise simulation, it is necessary to use inertial parameters, such as the mass, the location of the centre of mass, and the matrix of the moment of inertia, which will represent the UAV's rotational dynamics.

In the real world, the moment of inertia can be measured by using the bifilar pendulum method[7]. During testing, the UAV is suspended by two parallel non-flexible wires with known lengths that oscillate about the vertical axis due to the gravitational force. The mass moment of inertia is computed using measurements of the oscillation period and lengths of the pendulum wires.

However, it can be simplified to the cylinder inertial moment.

The moment of inertia for the cylinder for three axes can be calculated as follows:

$$X = \frac{m(3r^2 + h^2)}{12},$$

$$Y = \frac{m(3r^2 + h^2)}{12},$$

$$Z = \frac{mr^2}{2}.$$

Where m is the mass of the body, r is the radius of the cylinder, and h is the height of the cylinder.

Chapter 5

Experiments

To evaluate the reliability of the UAV, we held real-world experiments. The experiments included scenarios with strong wind, calm weather, and different configurations: using only leg supports, employing a gripper in conjunction with leg supports, and utilizing the gripper alone. As the racing platform is new for the MRS system, its profile after experiments and tuning was created. Furthermore, its model was added to the simulation in Gazebo.

5.1 Simulation

For visualisation of the UAV in the simulation, we created its detailed 3D model(5.1) in Fusion360[1].
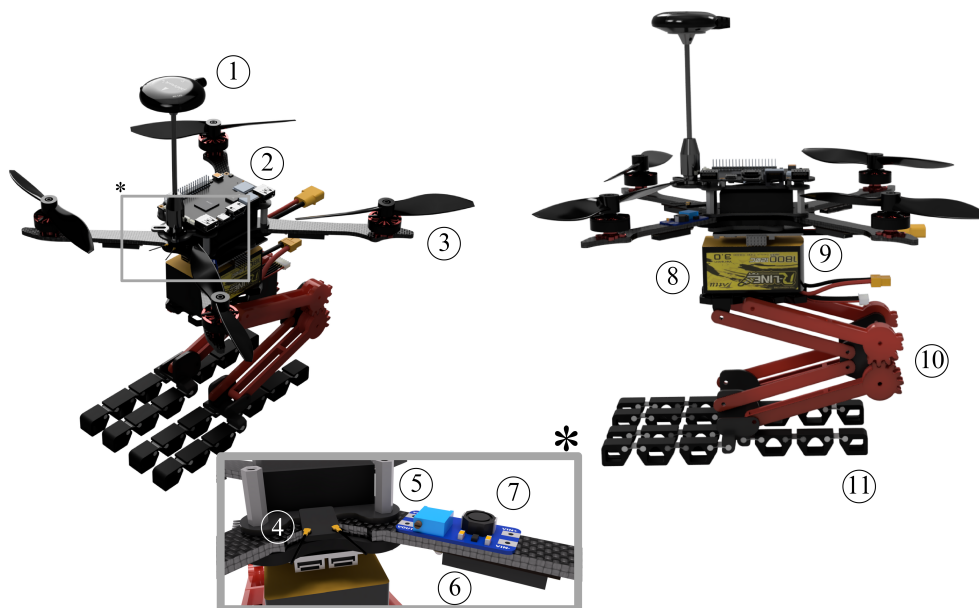

FIGURE 5.1: 3D model of UAV[2]: (1) M8N GPS module; (2) VIM4 Khadas; (3) HGLRC motors 2306.5 with 6 in propellers; (4) R81 Receiver; (5) Pixhawk 4 Mini; (6) ESC 40A; (7) Buck-Boost; (8) LiPo 1800mA 4 cell battery; (9) Power distribution board PM07; (10) 25 cm leg with tendon; (11) Gripper part.

---

[1] autodesk.com/products/fusion-360
[2] https://a360.co/3B15baQ

After it was successfully added as a model to the Gazebo simulation (5.2), some small parts, such as ESCs, Buck-Boost, etc., were omitted from the visualization. The UAV was then tested using test scripts, demonstrating its flight capabilities[3].
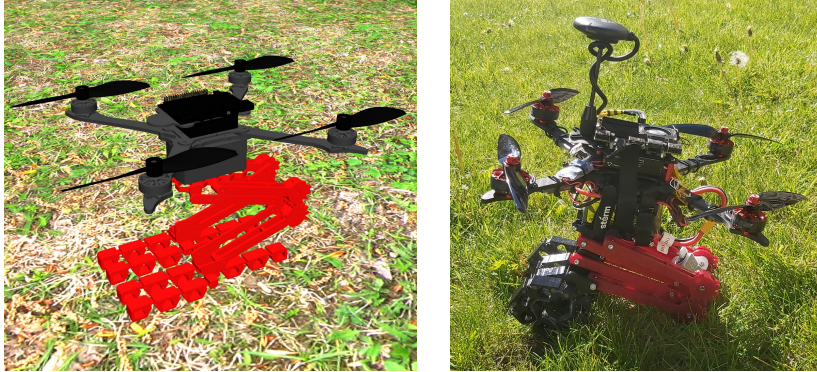

FIGURE 5.2: The UAV model in the Gazebo simulation environment and the UAV in the real world. The physics of legs is much more simplified: toes are not furled, legs are not fully bent; visualization of small components and sensors is omitted.
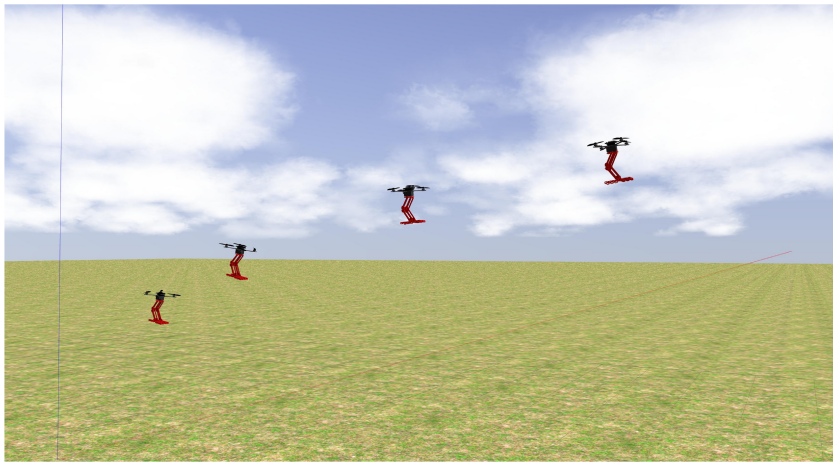

FIGURE 5.3: Four overlapping snapshots of the experiment of the UAV's flight in the Gazebo simulation environment

5.2 UAV flight testing

[3]https://youtube.com/shorts/5PJCvFSR_Sw?feature=share
[4]https://youtube.com/shorts/l-I8f9rom6U

(A)

(B)

FIGURE 5.4: UAV in real-world testing. (A) Landed state, legs bent; (B) Legs unbent during flight[4].

Weight with battery (g)	Weight of support legs (g)	Weight of gripper (g)
705	120	260
Flight time (min)	Propeller size (inch)	Battery voltage (V)
8	6	16.8

TABLE 5.1: Specifications of Final Version of UAV

During an autonomous flight with VIM4, we collected data on its performance. It showed a maximum 74.4% load when getting up, with approximately 52% average when just trying to preserve its position during wind, and 58% when commands to fly to a certain point were executed.

We flew UAV and changed its gains for SE(3) controller, and MPC tracker. Motor parameters that were calculated before were additionally recalculated after flight testing by adding different weights and testing hover thrusts values for them.

Before real-world testing, our calculated motor parameters were as follows:

$$a_t = 0.271 \quad b_t = -0.15.$$

After testing and tuning in flight we got:

$$a_t = 0.29398 \quad b_t = -0.24917.$$

Which differs by almost 0.1 for b_t, which can be due to an error in the calculation of hover thrust.

During the process of in-flight tuning, we collected data from the flight controller to analyze the UAV's performance[5]. Figures 5.5, 5.6, 5.7 show changes in angular rates (appendix B), when the UAV were flying. Pitches in graphs align with moving the UAV to the point in real life, which starts in the middle of the time axis. It can be seen that the first pitches were higher, but while tuning, the UAV started flying more smoothly and its tilt decreased.

---

[5]https://youtube.com/shorts/9rAElS2e2QQ?feature=share

FIGURE 5.5: Yaw rate response from Pixhawk4 during real flight.

FIGURE 5.6: Pitch rate response from Pixhawk4 during real flight.

FIGURE 5.7: Roll rate response from Pixhawk4 during real flight.

5.3 Gripper testing

As part of the modelling process, we designed two different versions of the legs, one with a 19 cm length and another 25 cm length(5.8). For testing, we attached them to the UAV and tried to see if the UAV creates enough force with its mass to close the gripper tightly.

As anticipated, small legs require more force to be bent, due to the limited torque generated. Thus the UAV was unable to close its legs fully, solely relying on the force produced by its mass, resulting in the UAV descending or falling down.

FIGURE 5.8: Comparison of the 25 cm leg and the 19 cm leg

Tests conducted with longer legs have demonstrated that the UAV is capable of closing its gripper using the force generated by its own mass. Furthermore, it can maintain a secure grip even when the pole is not entirely stable. However, the mass of the UAV must be fixed above the centre of the pole or with some shift towards the front in order to generate sufficient force to close the gripper and prevent the UAV from falling.
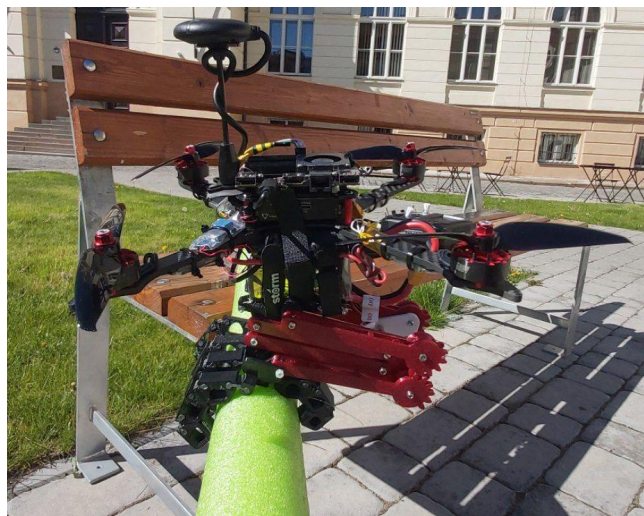

FIGURE 5.9: The UAV sitting using the gripper.

We increased friction force by adding rubber pads on each segment for better grip. That reduces the probability of the UAV falling from the stick due to its sliding.

During our test, we attempted to perch the UAV on the pole with a diameter of 65 mm. Our observations revealed, that tilting the UAV's body approximately 10 degrees forward during landing resulted in a tighter grip on the pole. However, we also observed that the maximum forward tilt angle was limited to approximately 32 degrees. Beyond this point, the UAV lost its grip and failed to land successfully. This limitation can be attributed to the shifted centre of gravity caused by the size of the legs. The legs' design, with two toes in the front and one in the back, allowed for a backward tilt of 10 degrees. However, as the tilt increased further, the legs in the

rear began to unbend, leading to a loss of grip and a failed landing attempt.

We conducted experiments on perching UAV manually on the pole. As expected, the UAV had to perch either vertically or with a slight forward angle for the gripper to catch the pole. Due to the difficulty in precisely controlling during the manual flight, it is almost impossible to land the UAV on the centre of the pole. Therefore, autonomous landing with visual sensors, such as cameras, which provide precision to cm, can deal with this problem.

Chapter 6

Conclusion and future work

6.1 Conclusion

In this work, we designed a new UAV, which weighs only 965 grams, with a passive perching mechanism.

From the software side, we added the UAV model to the simulation for experiments with its behaviour, with legs or without them. Furthermore, we successfully integrated the UAV into the MRS system, enabling autonomous flight.

Real-life experiments were held, even in challenging weather conditions such as strong winds. During experiments, we tuned the UAV's controller and tracker gains. The UAV demonstrated excellent performance by maintaining its position despite the wind. Moreover, the UAV showed precise flight capabilities when equipped with long legs.

All resources are available on GitHub[1].

6.2 Future work

Our results showed the potential for further improvement of the developed UAV. For future work, we want to continue improving the gripping mechanism. One potential improvement is to add a lock mechanism that would provide additional stability once the UAV has successfully perched and fixated itself onto the pole.

Further, we plan to integrate a camera for pole localization. That would enable autonomous perching, as the camera would provide data for precise positioning and alignment during the perching process.

Once these steps are implemented, we will be ready to proceed with testing our UAV for perching on another UAV.

We will also continue working with the developed UAV in other projects, without the use of legs.

---

[1]https://github.com/Diana-Doe/bachelor_work/tree/main

Appendix A

MPC and SE(3) controllers

Symbol	Meaning
f_d	desired thrust force produced by a controller [N]
m_e	mass error, the difference between real and calculated mass [kg]
e_p	steady-state control error in the position
e_v	velocity control error
$\ddot{r}_d$	desired acceleration in the world frame, 2nd derivative of position [ms^{-2}]
g	gravity constant [ms^{-2}]
d_w	world disturbance force term [ms^{-2}]
d_b	body disturbance force term [ms^{-2}]
k_p	position gains
k_v	velocity gains
c_d	desired acceleration $\in^3$

TABLE A.1: Appendix symbols

All provided formulas are used in the MRS system and are taken from [1]. Both MPC and SE(3) are used to find desired force and are interchangeable depending on the purpose.

A.0.1 SE(3)

For finding desired force SE(3) geometric tracking feedback with the addition of disturbance compensation is used:

$$f_d = -m_e k_p \circ e_p + -m_e k_v \circ e_v + m_e \ddot{r}_d + m_e g \hat{e}_3 + -d_w \circ \begin{bmatrix} 1 \\ 1 \\ 0 \end{bmatrix} + -d_b \circ \begin{bmatrix} 1 \\ 1 \\ 0 \end{bmatrix}.$$

Where the first two terms are position feedback and velocity feedback, the third is reference feedforward, the fourth is gravity compensation, and the fifth and the sixth are world and body disturbance compensation.

A.0.2 MPC

Linear MPC is a reliable feedback technique suitable for systems with known models. Using MPC desired force can be determined:

$$f_d = m_e \ddot{r}_d + m_e c_d + m_e g \hat{e}_3 + -d_w \circ \begin{bmatrix} 1 \\ 1 \\ 0 \end{bmatrix} + -d_b \circ \begin{bmatrix} 1 \\ 1 \\ 0 \end{bmatrix}.$$

Where the first term is reference feedforward, the second is MPC feedforward, the third is gravity compensation, and the fourth and the fifth are world and body disturbance compensation.
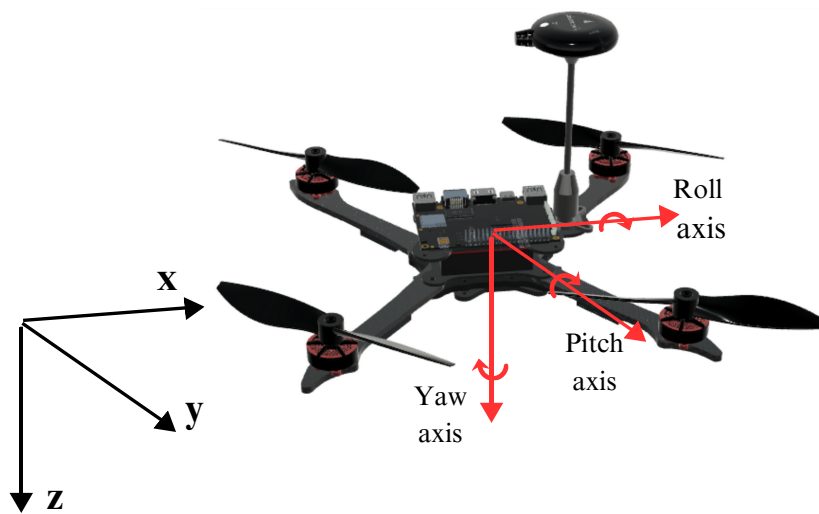
Appendix B

UAV axes

FIGURE B.1: The employed coordinate frames.

Bibliography

[1]   Tomas Baca et al. "The MRS UAV system: Pushing the frontiers of reproducible research, real-world deployment, and education with autonomous unmanned aerial vehicles". en. In: *J. Intell. Robot. Syst.* 102.1 (May 2021). DOI: 10.1007/s10846-021-01383-5.

[2]   Courtney E. Doyle et al. "An Avian-Inspired Passive Mechanism for Quadrotor Perching". In: *IEEE/ASME Transactions on Mechatronics* 18.2 (2013), pp. 506–517. DOI: 10.1109/TMECH.2012.2211081.

[3]   Peter Galton and Jeffrey Shepherd. "Experimental Analysis of Perching in the European Starling (Sturnus vulgaris: Passeriformes; Passeres), and the Automatic Perching Mechanism of Birds". In: *Journal of experimental zoology. Part A, Ecological genetics and physiology* 317 (Apr. 2012), pp. 205–15. DOI: 10.1002/jez.1714.

[4]   Daniel Hert et al. "MRS Modular UAV Hardware Platforms for Supporting Research in Real-World Outdoor and Indoor Environments". In: June 2022. DOI: 10.1109/ICUAS54217.2022.9836083.

[5]   Dariusz Horla et al. "AL-TUNE: A Family of Methods to Effectively Tune UAV Controllers in In-flight Conditions". In: *Journal of Intelligent and Robotic Systems* 103 (Sept. 2021), p. 5. DOI: 10.1007/s10846-021-01441-y.

[6]   Karan P. Jain and Mark W. Mueller. "Flying batteries: In-flight battery switching to increase multirotor flight time". In: *2020 IEEE International Conference on Robotics and Automation (ICRA)*. 2020, pp. 3510–3516. DOI: 10.1109/ICRA40945.2020.9197580.

[7]   Matthew Jardin and Eric Mueller. "Optimized Measurements of UAV Mass Moment of Inertia with a Bifilar Pendulum". In: *Journal of Aircraft - J AIRCRAFT* 46 (May 2009), pp. 763–775. DOI: 10.2514/1.34015.

[8]   George P. Kontoudis et al. "An Adaptive Actuation Mechanism for Anthropomorphic Robot Hands". In: *Frontiers in Robotics and AI* 6 (2019). ISSN: 2296-9144. DOI: 10.3389/frobt.2019.00047. URL: https://www.frontiersin.org/articles/10.3389/frobt.2019.00047.

[9]   Alexis Lussier Desbiens and Mark R Cutkosky. "Landing and perching on vertical surfaces with microspines for small unmanned air vehicles". en. In: *J. Intell. Robot. Syst.* 57.1-4 (Jan. 2010), pp. 313–327. DOI: 10.1007/s10846-009-9377-z.

[10] Raymond R. Ma, Joseph T. Belter, and Aaron M. Dollar. "Hybrid Deposition Manufacturing: Design Strategies for Multimaterial Mechanisms Via Three-Dimensional Printing and Material Deposition". In: *Journal of Mechanisms and Robotics* 7.2 (May 2015). 021002. ISSN: 1942-4302. DOI: 10.1115/1.4029400. eprint: https://asmedigitalcollection.asme.org/mechanismsrobotics/article-pdf/7/2/021002/6252283/jmr_007_02_021002.pdf. URL: https://doi.org/10.1115/1.4029400.

[11] Andrew McLaren et al. "A Passive Closing, Tendon Driven, Adaptive Robot Hand for Ultra-Fast, Aerial Grasping and Perching". In: *2019 IEEE/RSJ International Conference on Intelligent Robots and Systems (IROS)*. 2019, pp. 5602–5607. DOI: 10.1109/IROS40897.2019.8968076.

[12] Lorenz Meier et al. "PIXHAWK: A system for autonomous flight using on-board computer vision". In: *2011 IEEE International Conference on Robotics and Automation*. 2011, pp. 2992–2997. DOI: 10.1109/ICRA.2011.5980229.

[13] Jiawei Meng et al. "On aerial robots with grasping and perching capabilities: A comprehensive review". en. In: *Front. Robot. AI* 8 (2021). DOI: 10.3389/frobt.2021.739173.

[14] Ryo Miyazaki et al. "Airborne Docking for Multi-Rotor Aerial Manipulations". In: *2018 IEEE/RSJ International Conference on Intelligent Robots and Systems (IROS)*. 2018, pp. 4708–4714. DOI: 10.1109/IROS.2018.8594513.

[15] Paul M Nadan et al. "A bird-inspired perching landing gear System1". en. In: *J. Mech. Robot.* 11.6 (Dec. 2019), pp. 1–43. DOI: 10.1115/1.4044416.

[16] Morgan T. Pope et al. "A Multimodal Robot for Perching and Climbing on Vertical Outdoor Surfaces". In: *IEEE Transactions on Robotics* 33.1 (2017), pp. 38–48. DOI: 10.1109/TRO.2016.2623346.

[17] Pornthep Preechayasomboon and Eric Rombokas. "Negshell casting: 3D-printed structured and sacrificial cores for soft robot fabrication". In: *PLoS ONE* 15 (June 2020). DOI: 10.1371/journal.pone.0234354.

[18] W. R. T. Roderick, M. R. Cutkosky, and D. Lentink. "Bird-inspired dynamic grasping and perching in arboreal environments". In: *Science Robotics* 6.61 (2021). DOI: 10.1126/scirobotics.abj7562.

[19] William RT Roderick et al. "Birds land reliably on complex surfaces by adapting their foot-surface interactions upon contact". In: *eLife* 8 (2019). Ed. by Stanislav Gorb, Diethard Tautz, and Andrew Biewener, e46415. ISSN: 2050-084X. DOI: 10.7554/eLife.46415.

[20] David Saldaña et al. "ModQuad: The Flying Modular Structure that Self-Assembles in Midair". In: 2018. DOI: 10.1109/ICRA.2018.8461014.

[21] Martin Saska et al. "Vision-based high-speed autonomous landing and cooperative objects grasping - towards the MBZIRC competition". In: Dec. 2016.